

A Method of Fundamental Solutions for the One-dimensional Inverse Cauchy-Stefan Problem

Mohammed Baati, Mohamed Louzar and Abdellah Lamnii

Abstract—The main focus of our study is the one-dimensional parabolic Cauchy-Stefan inverse problem, which entails the identification of initial condition data. In this context, we explore the application of the method of fundamental solutions. This method is employed iteratively until the optimal initial condition data is determined. It generates an ill-conditioned matrix, which can be addressed through different regularization methods. Our numerical experiments and theoretical analyses of these approaches illustrate that accurate results can be achieved.

Index Terms—inverse Cauchy-Stefan problem, method of fundamental solutions, Tikhonov regularization, randomized singular value decomposition.

I. INTRODUCTION

THERE are three types of inverse mathematical physics problems: coefficient inverse problems, boundary inverse problems, and evolutionary inverse problems, each of which is concerned with recovering some equation coefficients, boundary conditions, and initial conditions [1]. They are often ill-posed, and solving them requires the employment of appropriate methods for developing stable solutions. During the last two decades, the authors worked to develop more precise techniques [2].

A specific manifestation of these challenges arises in complex or irregular domains. For instance, the problem is named after the slovenian physicist jozef Stefan, who defined the general class of such problems, and it can manifest in various formulations. It has relevance in numerous technical applications, such as ice melting, metal solidification, casting, and ablation.

The direct problem consists of calculating the temperature distribution and a function that describes the position of the moving boundary interface, while the inverse problem consists of calculating the temperature distribution as well as reconstructing the function that describes the temperature distribution on the boundary when the position of the moving interface (freezing front) is known [3]. The inverse Cauchy-Stefan problem, which corresponds to both the boundary and evolutionary inverse problem classifications, is the subject of this article [4].

Numerous studies on various types of free boundary problems have been conducted, both theoretically and numerically [5], [6]. However, these numerical approaches have the disadvantage of necessitating domain or boundary discretization, which becomes challenging for moving boundary problems, such as the Stefan problems discussed here. The meshless

approach to fundamental solutions (MFS), which does not require domain or boundary discretization, was recently implemented.

The method of fundamental solutions (MFS) is a complex numerical approach that is meshless, simple to use, and has a low computing cost compared to other frequent numerical methods [7], [8]. This approach can be used for both direct and inverse problems.

The authors of this paper have recently obtained numerical solutions for the inverse Stefan problem utilizing an MFS with boundary data recreated on the fixed boundary given the initial conditions and the moving interface [9].

The inverse Cauchy-Stefan problem is the inverse problem of determining the initial data. We applied the MFS to the inverse Cauchy-Stefan problem and compared the numerical reconstructions obtained here with those obtained here when the initial condition was not specified.

Our key contribution is to offer a framework to construct a fundamental solution method based on rSVD and to demonstrate the robustness of this method for solving problems. For comparison, we will compare this method to a popular Tikhonov regularization technique [10], [11], [12], [13].

This article is organized as follows: We present a mathematical formulation for the inverse Cauchy-Stefan problem in section 2. Section 3 describes an MFS approximation for this problem. In section 4, we discuss various regularization methods. Section 5 presents and examines four numerical examples that demonstrate the accuracy of the initial condition of the MFS for the inverse Cauchy-Stefan problem.

II. THE INVERSE CAUCHY-STEFAN PROBLEM

We have considered a one-dimensional, one-phase inverse Cauchy-Stefan problem. The moving boundary, which we take to be sufficiently smooth, is given by $x=f(t)$, for $0 < t \leq T$, where T is the given final positive time. We assume that $f(t) > 0$ for $t \in (0, T]$ and $f(0) \geq 0$. The heat conduction domain is $D_w = (0, f(t)) \times (0, T]$ with closure $\bar{D}_w = [0, f(t)] \times [0, T]$.

For the inverse Cauchy-Stefan problem, we attempt to determine the solution $w(x, t)$ and the moving boundary given by $x=f(t)$, verifying the heat equation

$$\frac{\partial w}{\partial t}(x, t) - \frac{\partial^2 w}{\partial x^2}(x, t) = 0, (x, T) \in D_w \quad (1)$$

The dirichlet and neumann conditions on the moving boundary $f(t)$ are given below

$$w(f(t), t) = k_1(t), t \in (0, T] \quad (2)$$

$$\frac{\partial w}{\partial x}(f(t), t) = k_2(t), t \in (0, T] \quad (3)$$

In Stefan problems, usually $k_1(t)=0$ and $k_2(t)=-f'(t)$.

Manuscript received December 17, 2023; revised September 29, 2024.

Mohammed Baati is a PhD student at Hassan First University of Settat, FST, MISI Lab, Settat, Morocco (e-mail: m.baati@uhp.ac.ma)

Mohamed Louzar is a professor at Hassan First University of Settat, FST, MISI Lab, Settat, Morocco (mohamed.louzar@uhp.ac.ma)

Abdellah Lamnii is a professor at Abdelmalek Essaadi University, LaSAD, ENS, 93030, Tetouan, Morocco (e-mail: a.lamnii@uae.ac.ma)

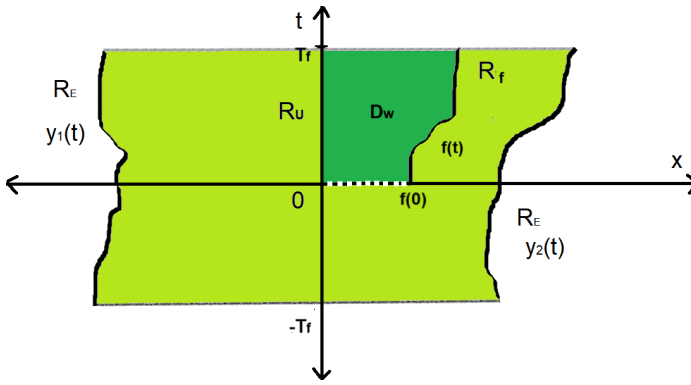


Fig. 1. The domain is generally represented D_w , boundary $R=R_u \cup R_f$, and source points placed on y_1 and y_2 external to the domain D_w .

We then need to find the initial condition of the solution at $t=0$, i.e. determine $w_0(x)$ with

$$w(x, 0) = w_0(x), x \in (0, f(0)] \quad (4)$$

$$w(0, t) = k(t), x \in (0, T] \quad (5)$$

$$\frac{\partial w}{\partial x}(0, t) = G(t), t \in (0, T] \quad (6)$$

The existence, uniqueness, and continuous data dependence of a solution are defined in [14], [15]. The remainder of this work examines the inverse Cauchy-Stefan problem, which involves determining the temperature $w(x,t)$ that satisfies equations (1)–(3), assuming a given $f(t)$. This study allowed us to determine the unknown initial conditions. The ill-posed nature of the problem was resolved, and the convergence was enhanced using the method of fundamental solutions with rSVD regularization.

III. THE METHOD OF FUNDAMENTAL SOLUTIONS (MFS)

MFS has become more popular in recent years as a numerical method for solving linear partial differential equations (PDEs) with an explicit fundamental solution. The MFS has been widely used to solve elliptic linear PDEs such as the biharmonic, Laplace, Lamé, Helmholtz, convection-diffusion, and Stokes equations, but it has only recently been extended to parabolic linear PDEs such as the heat equation [16], [17].

We present the fundamental solutions of the one-dimensional heat equation Eq.(1) see [16]

$$G(x, t, y, \theta) = \frac{H(t - \theta)}{(4\pi(t - \theta))^{\frac{1}{2}}} e^{-\frac{(x-y)^2}{4(t-\theta)}} \quad (7)$$

where H denotes the heaviside function.

We have constructed a new version of the method for approximating the fundamental solutions of (1)-(3) by a linear combination of the fundamental solutions (7) obtained by

$$w_\infty(x, t) = \sum_{j=1}^2 \sum_{m=1}^{\infty} c_m^j G(x, t, y_j(\theta_m), \theta_m), (x, t) \in \bar{D}_w \quad (8)$$

To implement the fundamental solutions method for the inverse Cauchy-Stefan problem, we truncate (8) by considering a finite number of terms, namely

$$w_M(x, t) = \sum_{j=1}^2 \sum_{m=1}^{2M} c_m^j G(x, t, y_j(\theta_m), \theta_m), (x, t) \in \bar{D}_w \quad (9)$$

c_m^j are real coefficients that must be determined. In addition, $\{y_i\}_{i=1}^2=1$ are external space singularities $[0, f(t)]$, $t \in [0, T]$ and $\{\theta_j\}_{j=1}^M=1$ are time singularities that exist in the interval $(-T, T)$.

To construct the MFS matrix, we must first distribute the source and collocation points. We place the first four examples presented in figure 2. The source points are placed at

$$(-L, \theta), \theta \in (-T, T)$$

$$(f(\theta) + L, \theta), \theta \in (0, T)$$

$$(f(0) + L, \theta), \theta \in (-T, 0)$$

$$y_1(\theta) = -L, y_2(\theta) = L + f(\theta_j H(\theta_j)), j = 1, \dots, M + 1$$

Where the time points $\{\theta_j\}_{j=1, \dots, M+1} \in (-T, T)$ are given by

$$\theta_{\frac{M}{2}+1-m} = -\frac{T}{2M} - \frac{2T}{M+1}m, m = 0, \dots, \frac{M}{2}$$

$$\theta_{\frac{M}{2}+2+m} = \frac{3T}{2M} + \frac{2T}{M}m, m = 0, \dots, \frac{M}{2} - 1$$

However, for the collocation points, we let

$$t_i = \frac{i}{M}T, x_1^i = f(t_i), i = 0, \dots, M$$

Equations (2) and (3) are used at the collocation points to determine the coefficients c_i^j . The outcomes of the equations are as follows:

$$w_M(x_1^i, t_i) = 0, i = 0, \dots, M \quad (10)$$

$$\frac{\partial w_M}{\partial x}(x_1^i, t_i) = -f'(t_i), i = 0, \dots, M \quad (11)$$

The number of equations in the system of equations (10) and (11) is the same as the number of unknowns, or $2(M+1)$.

The collocated data from the boundary is required for MFS to compute the solution. Then, we include random noise to (3) in the form of

$$w_x^\delta(f(t), t) = w_x(f(t), t) + N(0, (\sigma^\delta)^2) \quad (12)$$

where

$$\sigma^\delta = \delta \times \max_{(f(t), t), t \in (0, T)} |w_x(f(t), t)| \quad (13)$$

$N(0, (\sigma^\delta)^2)$ denotes random noise, i.e., the normal distribution with zero mean and standard deviation σ^δ , where σ indicates the percentage of relative random noise.

Finally, the equation system can be presented as

$$Ac = g \quad (14)$$

Where matrix A represents the value of the MFS solution at the collocation and source points, c is the vector of unknown constants c_j^i , and g is the vector defining the values at the collocation points.

The matrix A contains a large number of conditions, we must use regularization methods such as Tikhonov regularization and randomized singular value decomposition to produce a more efficient regularization [18], [19], [20].

IV. REGULARIZATION METHODS

Regularization methods are essential for the solution of the ill-conditioned linear system. The Tikhonov regularization method of ill-posed problems seeks to redefine the concepts of inversion and approximate solution so that the regularized solution developed by regularized inversion depends continuously on the data and corresponds to the exact solution. In its simplest form, Tikhonov regularization changes the linear system (14) with the regularized system given as follows.

$$(A^T A + \alpha I)c = A^T g \quad (15)$$

A^T represents the transpose of the matrix A , I represents the identity matrix, and $\alpha \geq 0$ represents the regularization parameter.

In this paper, we use randomized SVD methods to study the acceleration of an ill-conditioned linear system.

Randomized algorithms have demonstrated their efficacy in solving the ill-conditioned linear system [21]. Another approach is to use random to identify the subspace of the dominant matrix A . This is accomplished by multiplying A by a random matrix on its right or left side, and then obtaining the orthonormal basis matrix Q of the subspace.

A low-rank approximation of A can be computed using Q , giving the estimated truncated SVD. Because the dimension of the subspace is significantly smaller than that of $\text{range}(A)$, this method makes it simpler to compute near-optimal A decompositions. The algorithm presents a basic randomized SVD (rSVD) [22], [23], [24]:

- **Input:** $A \in R^{m \times n}$, rank parameter k , power parameter p
- **Output:** $U \in R^{m \times k}$, $S \in R^{k \times k}$, $V \in R^{n \times k}$
- $\Omega = \text{randn}(n, k+s)$
- $Q = \text{orth}(A\Omega)$
- for $i = 1, 2, \dots, p$ do
- $G = \text{orth}(A^T Q)$
- $Q = \text{orth}(AG)$
- end
- $B = Q^T A$
- $[U, S, V] = \text{svd}(B)$
- $U = QU$
- $U = U(:, 1:k)$, $S = S(1:k, 1:k)$, $V = V(:, 1:k)$.

We use gaussian elimination to solve this well-conditioned, linear system of equations for the coefficients of c [25].

V. NUMERICAL RESULTS

A. Example 1

We will commence by examining example 1 from reference [26], wherein the initial data are unspecified. It becomes evident that the free boundary is delineated by the linear function.

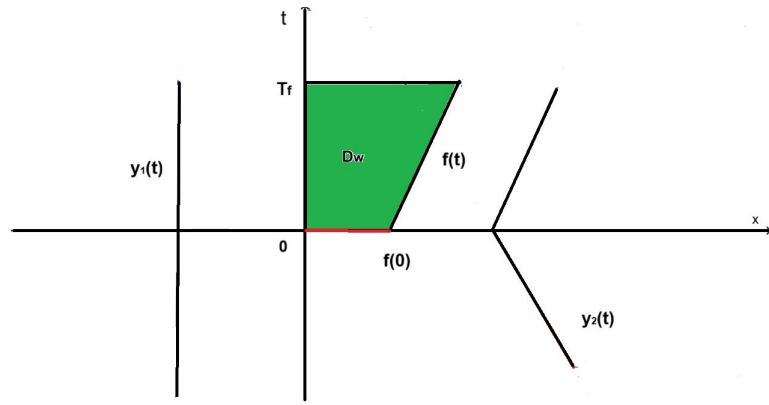


Fig. 2. Particularisation of Fig.1 for example 1, example 2 and example 3.

$$f(t) = \sqrt{2} - 1 + \frac{t}{\sqrt{2}}, t \in [0, T = 1] \quad (16)$$

We position the source points, as defined by equation (13), along the external boundaries $(-L, \theta)$, $\theta \in (-1, 1)$, $(f(\theta) + L, \theta)$, $\theta \in [0, 1)$ and $(f(0) + L, \theta)$, $\theta \in (-1, 0)$; For a graphical representation, refer to figure 2. We then apply the solution of the heat equation in the domain D_w , depicted by

$$w(x, t) = -1 + \exp\left(1 - \frac{1}{\sqrt{2}} + \frac{t}{2} - \frac{x}{\sqrt{2}}\right), (x, t) \in [0, f(t)] \times [0, 1] \quad (17)$$

We establish the subsequent boundary conditions at the moving boundary

$$w(f(t), t) = 0, t \in (0, 1] \quad (18)$$

$$\frac{\partial w}{\partial x}(f(t), t) = -f'(t) = -\frac{1}{\sqrt{2}}, t \in (0, 1] \quad (19)$$

Random additive noise is introduced into the neumann data (18) as described below

$$w_x^\delta(f(t), t) = -\frac{1}{\sqrt{2}} + N(0, \delta^2) \quad (20)$$

Where $N(0, \delta^2)$ corresponds to the normal distribution with mean zero and standard deviation

$$\sigma = \delta \times \max_{(f(t), t), t \in (0, 1]} |w_x(f(t), t)| = \frac{\delta}{\sqrt{2}} \quad (21)$$

Where δ is the relative noise level.

We aim to determine the initial condition at $t=0$, denoted as

$$w(x, 0) = -1 + \exp\left(1 - \frac{1}{\sqrt{2}} - \frac{x}{\sqrt{2}}\right), x \in [0, f(0) = \sqrt{2} - 1] \quad (22)$$

We choose $\alpha = 10^{-6}$ for $\delta=1\%$ and $\delta=3\%$, $\alpha=10^{-5}$ for $\delta=5\%$, See [4].

The simulation parameters are outlined in table 1.

Figures 3 and 5 present plots of the MFS approximations for the reconstructed data $w(x, 0)$ corresponding to varying noise levels $\sigma=1\%$ and $\sigma=3\%$ with $\alpha=10^{-6}$, subsequently, figure 7 displays plots of the MFS approximations for the

TABLE I
THE SIMULATION CONDITIONS

Hardware or Software	Parameters
CPU	Intel(R) Core (TM) i7-10750H CPU
RAM	16 Go
Platform	MATLAB R2016a

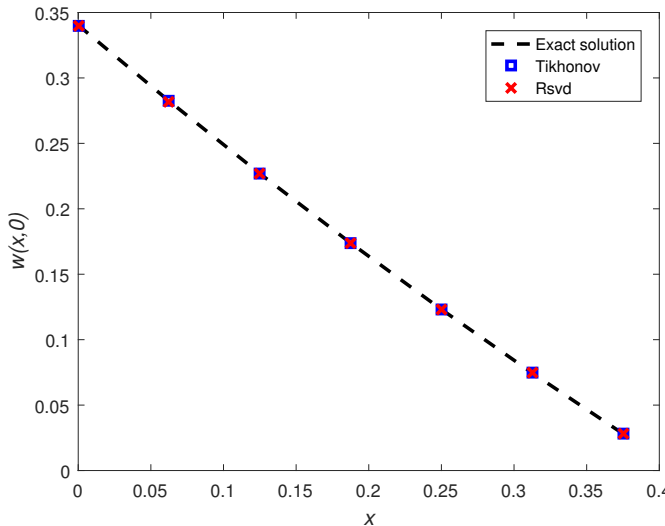


Fig. 3. The exact solution $w(x,0)$ and the MFS approximation with Tikhonov and rSVD established with $L=2$, $\alpha = 10^{-6}$, $k=30$, $M=16$ and $\delta=1\%$.

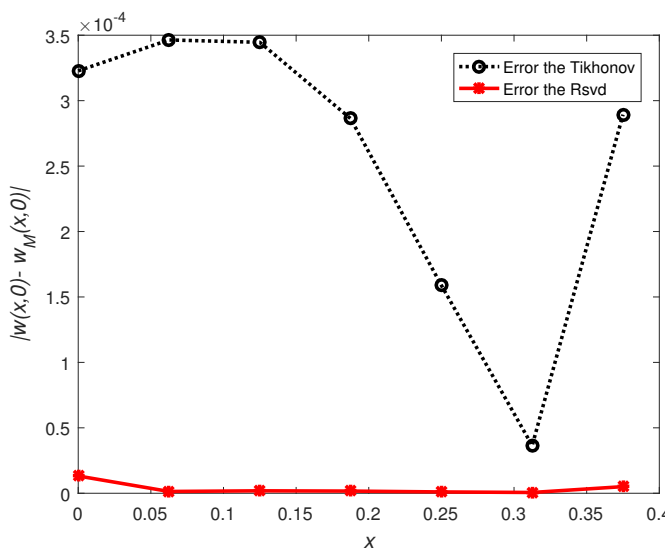


Fig. 4. Error between the exact solution $w(x,0)$ and the MFS approximation with Tikhonov and rSVD established with $\delta=1\%$.

reconstructed data $w(x,0)$ under the noise level $\sigma=5\%$ with $\alpha=10^{-5}$.

Figure 3 illustrates how to determine the initial condition using MFS, the rSVD regularization method, and the Tikhonov method. We added 1% additive noise to demonstrate the stability of these methods, and we observed that using MFS with the rSVD regularization method is more accurate than the exact solution.

Figure 5 illustrates that using MFS to find the initial condition with the rSVD regularization approach is more

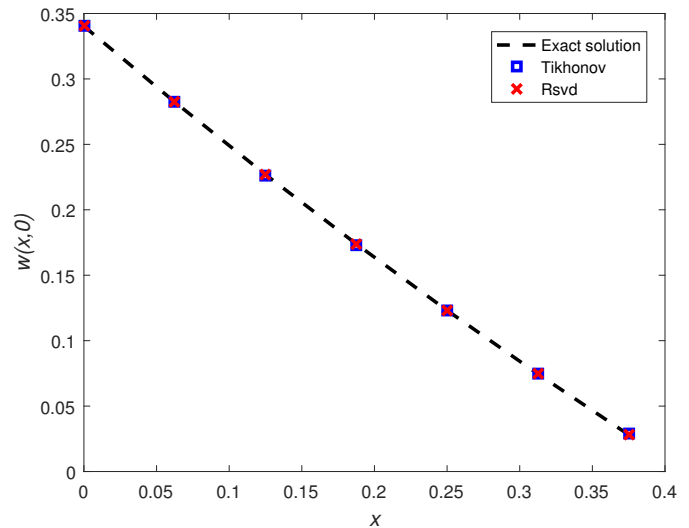


Fig. 5. The exact solution $w(x,0)$ and the MFS approximation with Tikhonov and rSVD established with $L=2$, $\alpha = 10^{-6}$, $k=30$, $M=16$ and $\delta=3\%$.

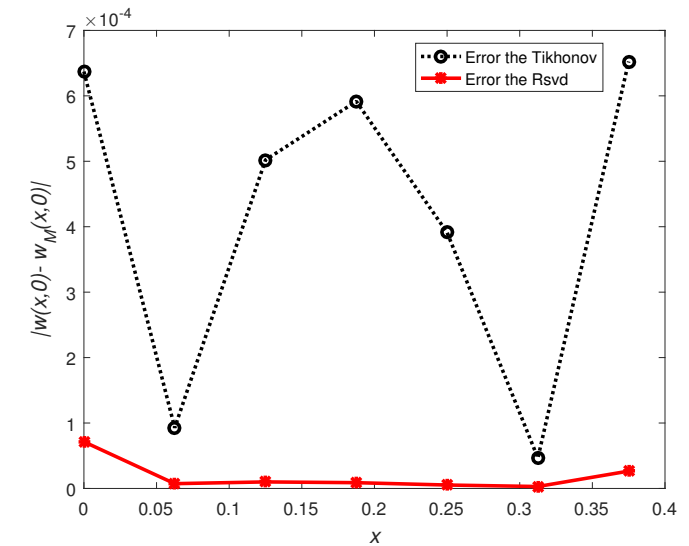


Fig. 6. Error between the exact solution $w(x,0)$ and the MFS approximation with Tikhonov and rSVD established with $\delta=3\%$.

accurate than the Tikhonov method when the additive noise is increased to 3%.

Figure 7 shows that MFS numerical results for finding the initial condition with rSVD regularization are more accurate than the Tikhonov method when the additive noise is 5%.

In this paper, we show that our results for the inverse Cauchy-Stefan problem outperform those in [4].

Figures 4, 6, and 8 demonstrate the difference between the exact solution and the MFS approximation using rSVD and Tikhonov regularization. We see that the method of fundamental solutions with rSVD regularization produces a smaller error than Tikhonov regularization. We can therefore determine that MFS with rSVD regularization produces more accurate and stable results than Tikhonov regularization at different additive noise levels.

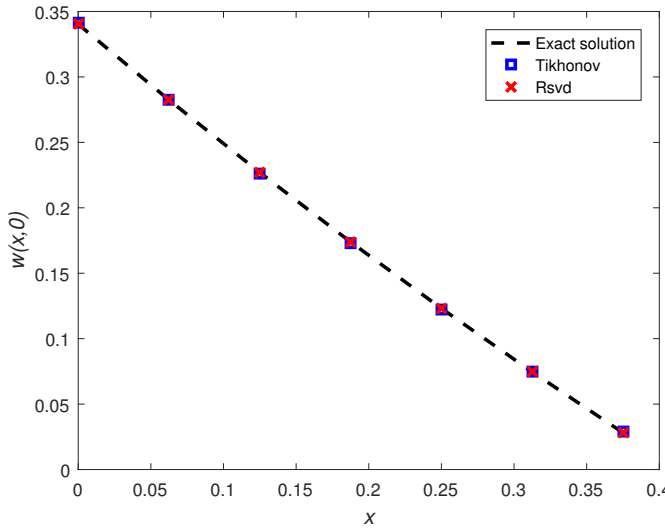


Fig. 7. The exact solution $w(x,0)$ and the MFS approximation with Tikhonov and rSVD established with $L=2$, $\alpha = 10^{-5}$, $k=30$, $M=16$ and $\delta=5\%$.

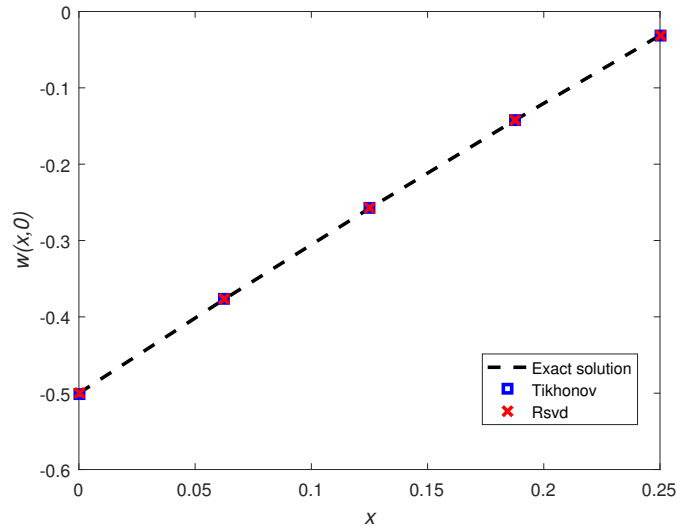


Fig. 9. The exact solution $w(x,0)$ and the MFS approximation with Tikhonov and rSVD established with $L=2.5$, $\alpha = 10^{-6}$, $k=30$, $M=16$ and $\delta=1\%$.

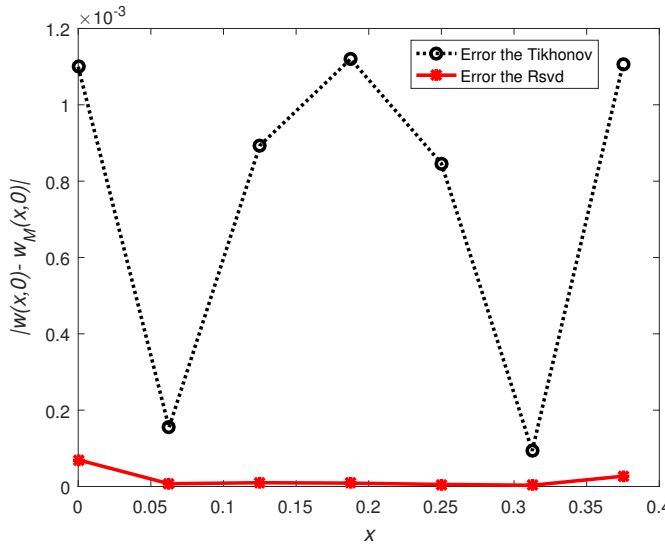


Fig. 8. Error between the exact solution $w(x,0)$ and the MFS approximation with Tikhonov and rSVD established with $\delta=5\%$.

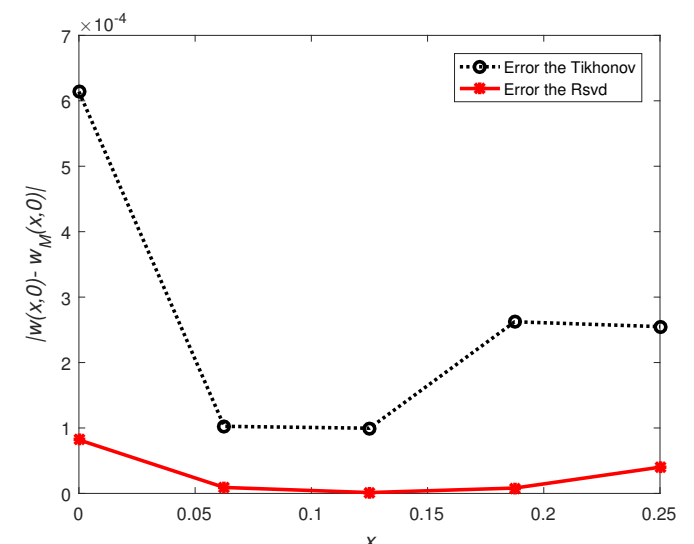


Fig. 10. Error between the exact solution $w(x,0)$ and the MFS approximation with Tikhonov and rSVD established with $\delta=1\%$.

B. Example 2

The second example uses a non-linear function to construct a moving boundary

$$f(t) = 2 - \sqrt{3 - 2t}, t \in [0, 1] \quad (23)$$

The source points are positioned on the external boundaries $(-L, \theta), \theta \in (-1, 1)$, $(f(\theta) + L, \theta), \theta \in (0, 1)$ and $(f(-\theta) + L, \theta), \theta \in (-1, 0)$. The exact solution is given by

$$w(x, t) = -\frac{x^2}{2} + 2x - \frac{1}{2} - t, (x, t) \in [0, f(t)] \times [0, 1] \quad (24)$$

In this example, the boundary conditions were as follows

$$w(f(t), t) = 0, t \in (0, 1] \quad (25)$$

$$\frac{\partial w}{\partial x}(f(t), t) = -f'(t) = \sqrt{3 - 2t}, t \in (0, 1] \quad (26)$$

Random additive noise, simulating measurement errors in the Neumann data (25), was introduced as

$$w_x^\delta(f(t), t) = \sqrt{3 - 2t} + N(0, \sigma^2), t \in (0, 1] \quad (27)$$

The dirichlet and neumann boundary conditions on the fixed boundary $x=0$ are as follows

$$w(0, t) = -\frac{1}{2} - t, t \in [0, 1] \quad (28)$$

$$\frac{\partial w}{\partial x}(0, t) = 2, t \in [0, 1] \quad (29)$$

We want to find the initial condition at $t=0$, given by

$$w(x, 0) = -\frac{x^2}{2} + 2x - \frac{1}{2}, x \in [0, f(0)], f(0) = 2 - \sqrt{3} \quad (30)$$

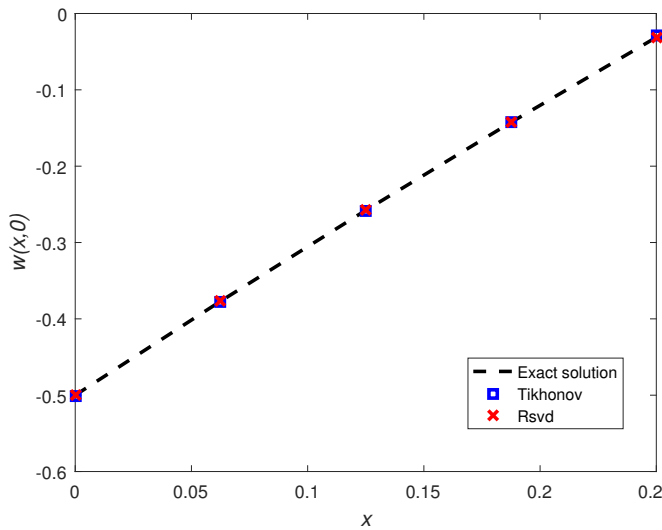


Fig. 11. The exact solution $w(x,0)$ and the MFS approximation with Tikhonov and rSVD established with $L=2.5$, $\alpha = 10^{-6}$, $k=30$, $M=16$ and $\delta=3\%$.

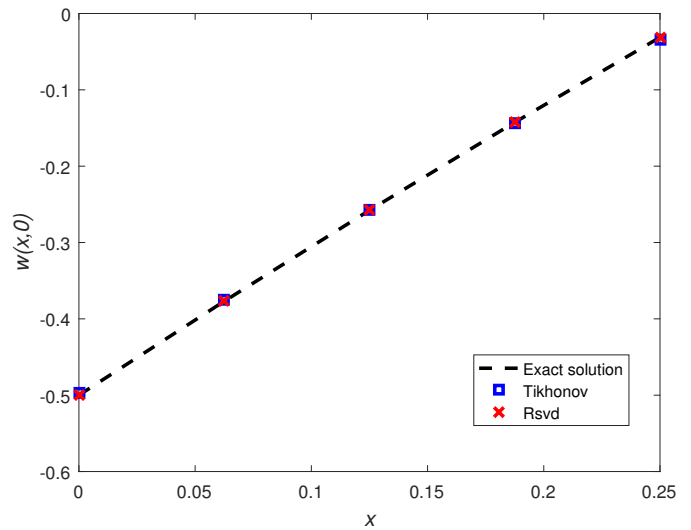


Fig. 13. The exact solution $w(x,0)$ and the MFS approximation with Tikhonov and rSVD established with $L=2.5$, $\alpha = 10^{-5}$, $k=30$, $M=16$ and $\delta=5\%$.

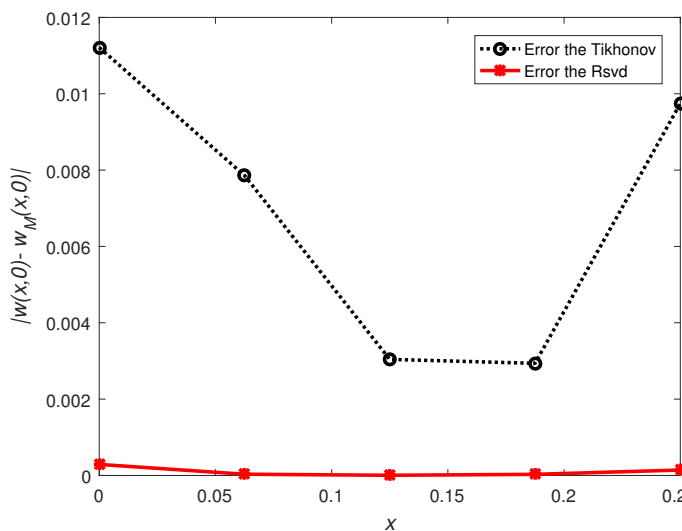


Fig. 12. Error between the exact solution $w(x,0)$ and the MFS approximation with Tikhonov and rSVD established with $\delta=3\%$.

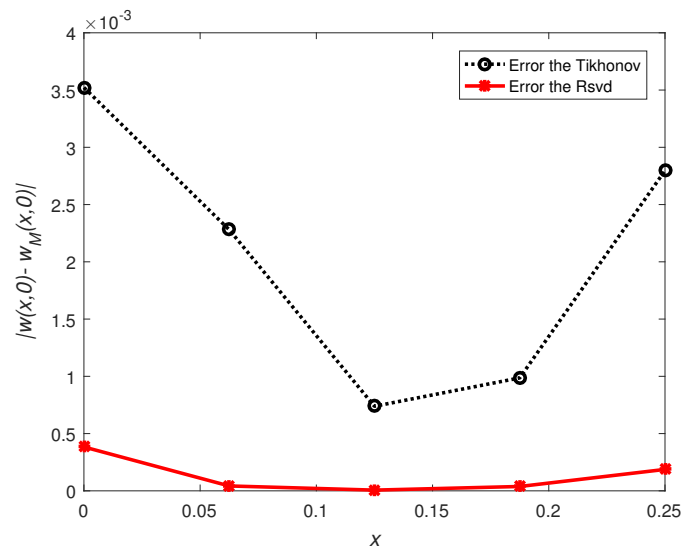


Fig. 14. Error between the exact solution $w(x,0)$ and the MFS approximation with Tikhonov and rSVD established with $\delta=5\%$.

Figure 9 shows a comparison of the MFS approximation with rSVD regularization and Tikhonov regularization against the exact solution with additive noise equal to 1%.

Figure 11 shows a comparison of the MFS approximation with rSVD regularization and Tikhonov regularization against the exact solution with additive noise equal to 3%.

In Figure 13, we increase the additive noise to 5%, illustrating a comparison of the MFS approximation with rSVD regularization and Tikhonov regularization against the exact solution.

Figures 10, 12, and 14 demonstrate that MFS with rSVD regularization is more accurate and stable than the Tikhonov method, even when additive noise increases. We observe that the error with rSVD regularization stays smaller than that with Tikhonov regularization.

C. Example 3

The linear function presents a moving boundary in this example [27]

$$f(t) = \frac{13}{4} - \left(\frac{81}{16} - 2t\right)^{1/2}, t \in [0, 1] \quad (31)$$

The source points are positioned on the external boundaries $(-L, \theta), \theta \in (-1, 1)$, $(f(\theta)+L, \theta), \theta \in (0, 1)$ and $(f(-\theta)+L, \theta), \theta \in (-1, 0)$. The exact solution is given by

$$w(x, t) = \left(x - \frac{13}{4}\right)^2 + 2\left(t - \frac{81}{32}\right), (x, t) \in [0, f(t)] \times [0, 1] \quad (32)$$

Such as this example has the following boundary conditions

$$w(f(t), t) = 0, t \in (0, 1] \quad (33)$$

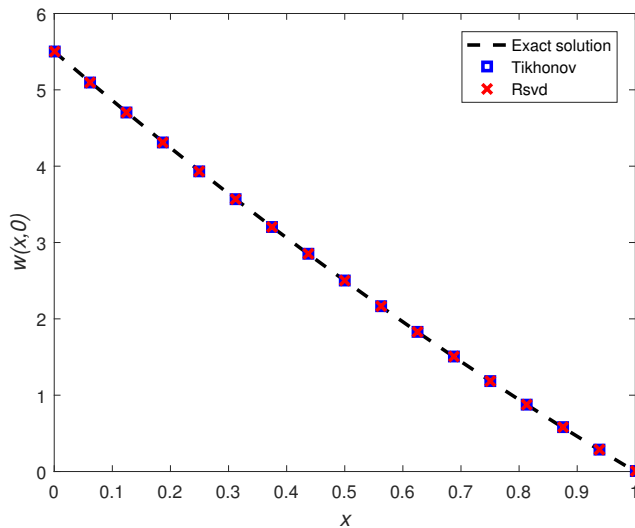


Fig. 15. The exact solution $w(x,0)$ and the MFS approximation with Tikhonov and rSVD established with $L=2.2$, $\alpha = 10^{-10}$, $k=30$, $M=16$ and $\delta=1\%$.

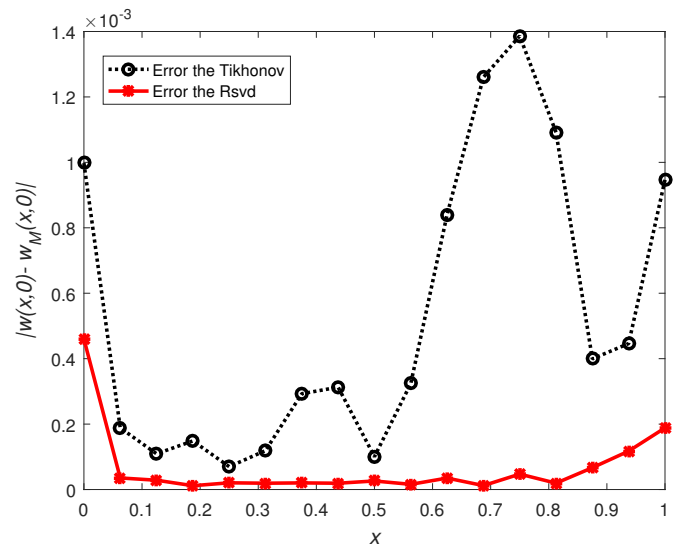


Fig. 16. Error between the exact solution $w(x,0)$ and the MFS approximation with Tikhonov and rSVD established with $\delta=1\%$.

$$\frac{\partial w}{\partial x}(f(t), t) = -f'(t) = \frac{13}{2} - 2\left(\frac{81}{16} - 2t\right)^{1/2}, t \in (0, 1] \quad (34)$$

Random additive noise simulating measurement errors to the neumann data (33) has been included as

$$w_x^\delta(f(t), t) = \frac{13}{2} - 2\left(\frac{81}{16} - 2t\right)^{1/2} + N(0, \sigma^2), t \in (0, 1] \quad (35)$$

The dirichlet and neumann boundary conditions on the fixed boundary $x=0$ are as follows:

$$w(0, t) = \frac{13^2}{4} + 2\left(t - \frac{81}{32}\right), t \in [0, 1] \quad (36)$$

$$\frac{\partial w}{\partial x}(0, t) = -\frac{13}{2}, t \in [0, 1] \quad (37)$$

We want to find the initial condition at $t=0$, given by

$$w(x, 0) = \left(x - \frac{13}{4}\right)^2 - \frac{81}{16}, x \in [0, f(0)], f(0) = 2 - \sqrt{3} \quad (38)$$

We have seen that the MFS approximation is shown in figure 15, figure 17, and figure 19 for finding initial conditions with parameter the regularization and three types of additive noise. These approximations show that rSVD regularization will be more accurate than the Tikhonov method.

Figures 16, 18 and 20 show that the rSVD method performs better and is more stable than the Tikhonov method when the regularization parameters are $\alpha=10^{-10}$.

D. Example 4

In this example, the exact solution is given by

$$w(x, t) = 1 - \frac{1}{3}x + t, (x, t) \in [0, f(t)] \times [0, 1] \quad (39)$$

and

$$f(t) = 3t + 3, t \in [0, 1] \quad (40)$$

Thence

$$w(f(t), t) = 0, t \in (0, 1] \quad (41)$$

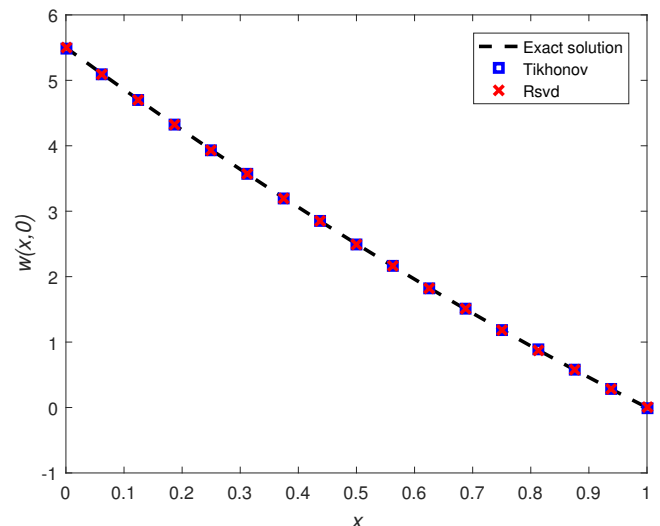


Fig. 17. The exact solution $w(x,0)$ and the MFS approximation with Tikhonov and rSVD established with $L=2.2$, $\alpha = 10^{-10}$, $k=30$, $M=16$ and $\delta=3\%$.

$$\frac{\partial w}{\partial x}(f(t), t) = -f'(t) = -\frac{1}{3}, t \in (0, 1] \quad (42)$$

Random additive noise and modeling measurement errors in neumann data (43) has been established as

$$w_x^\delta(f(t), t) = -\frac{1}{3} + N(0, \sigma^2), t \in (0, 1] \quad (43)$$

The dirichlet and neumann boundary conditions on the fixed boundary $x=0$ are as follows:

$$w(0, t) = 1 + t, t \in [0, 1] \quad (44)$$

$$\frac{\partial w}{\partial x}(0, t) = -\frac{1}{3}, t \in [0, 1] \quad (45)$$

We want to find the initial condition at $t=0$, which is given by

$$w(x, 0) = 1 - \frac{1}{3}x, x \in [0, f(0)], f(0) = 3 \quad (46)$$

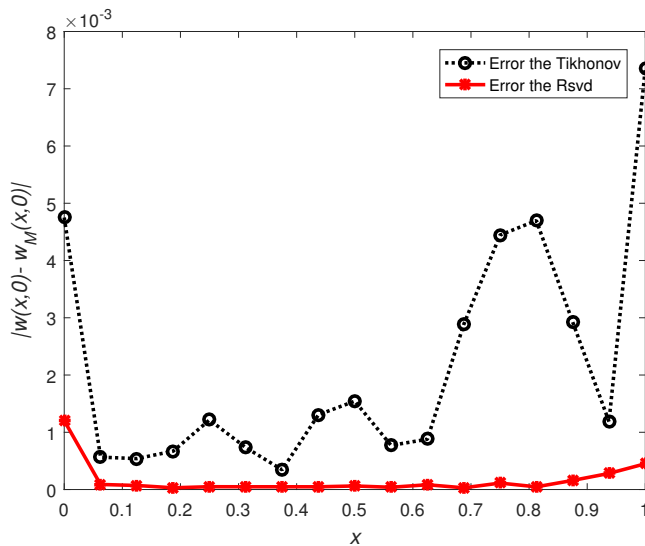


Fig. 18. Error between the exact solution $w(x,0)$ and the MFS approximation with Tikhonov and rSVD established with $\delta=3\%$.

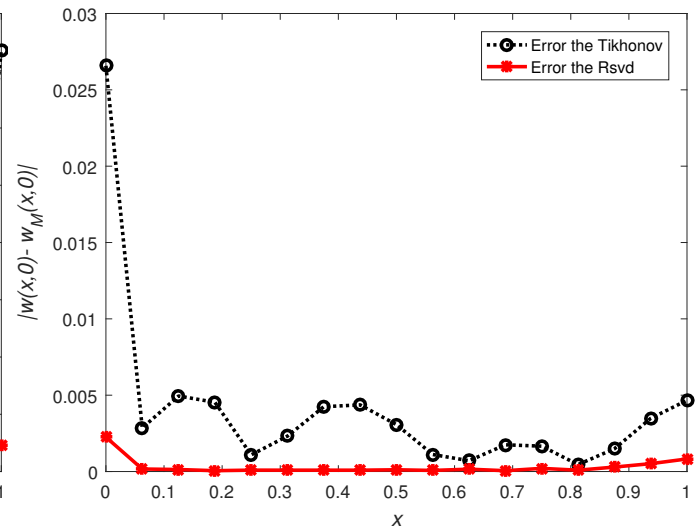


Fig. 20. Error between the exact solution $w(x,0)$ and the MFS approximation with Tikhonov and rSVD established with $\delta=5\%$.

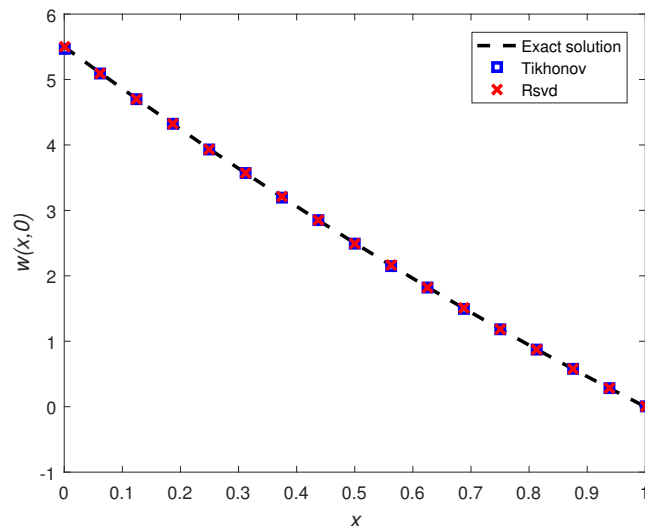


Fig. 19. The exact solution $w(x,0)$ and the MFS approximation with Tikhonov and rSVD established with $L=2.2$, $\alpha = 10^{-10}$, $k=30$, $M=16$ and $\delta=5\%$.

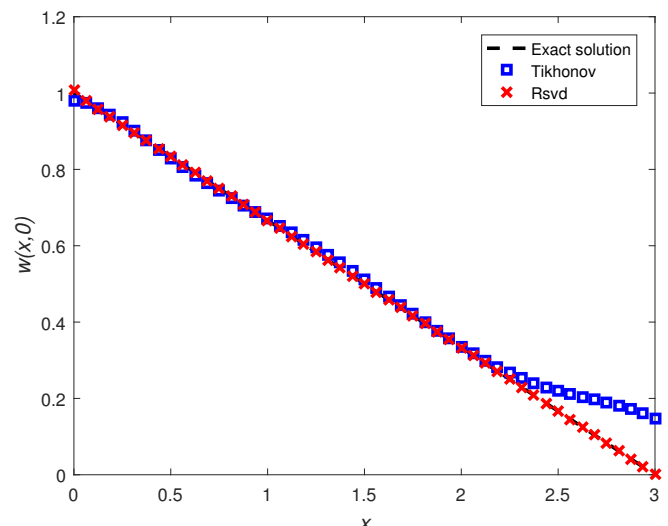


Fig. 21. The exact solution $w(x,0)$ and the MFS approximation with Tikhonov and rSVD established with $L=1.3$, $\alpha = 10^{-5}$, $k=30$, $M=26$ and $\delta=1\%$.

Figure 21 illustrates the MFS approximation to determine the initial condition using two methods of regularization rSVD and Tikhonov, and additive noise 1%, with the regularization parameter $\alpha=10^{-5}$.

Figure 23 illustrates the MFS approximation to find the initial condition using two methods of regularization rSVD and Tikhonov, and additive noise 3%, with regularization value $\alpha=10^{-5}$.

Figure 25 shows an MFS approximation for determining the initial condition based on rSVD and Tikhonov regularization, with 5% additive noise. The regularization parameter is $\alpha=10^{-4}$.

The results show that as the additive noise increases, the MFS approximation remains more accurate with rSVD regularization than with Tikhonov regularization.

Figures 22, 24, and 26 show that the error between the MFS approximation and the exact solution is small with the rSVD method compared to the Tikhonov method when the

regularization parameters are $\alpha=10^{-5}$ and $\alpha=10^{-4}$.

E. Example 5

In this example, the exact solution is given by

$$w(x, t) = -1 + \exp(t - x + 1), (x, t) \in [0, f(t)] \times [0, 1] \quad (47)$$

and

$$f(t) = t + 1, t \in [0, 1] \quad (48)$$

Thence

$$w(f(t), t) = 0, t \in (0, 1] \quad (49)$$

$$\frac{\partial w}{\partial x}(f(t), t) = -f'(t) = -1, t \in (0, 1] \quad (50)$$

Random additive noise and modeling measurement errors in neumann data (51) has been established as

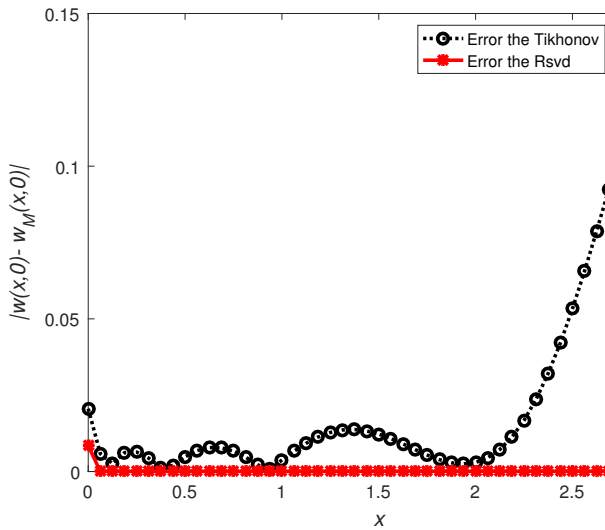


Fig. 22. Error between the exact solution $w(x,0)$ and the MFS approximation with Tikhonov and rSVD established with $\delta=1\%$.

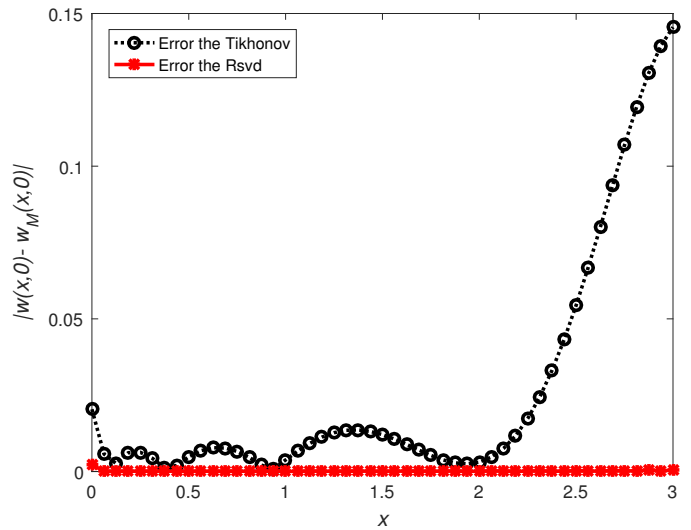


Fig. 24. Error between the exact solution $w(x,0)$ and the MFS approximation with Tikhonov and rSVD established with $\delta=3\%$.

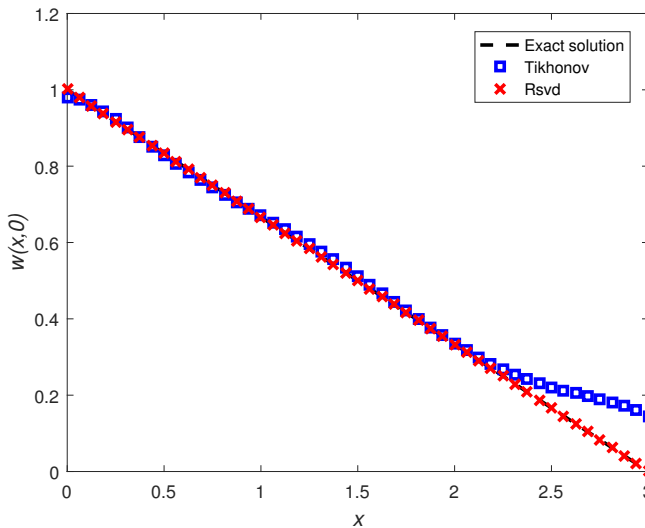


Fig. 23. The exact solution $w(x,0)$ and the MFS approximation with Tikhonov and rSVD established with $L=1.3$, $\alpha = 10^{-5}$, $k=30$, $M=26$ and $\delta=3\%$.

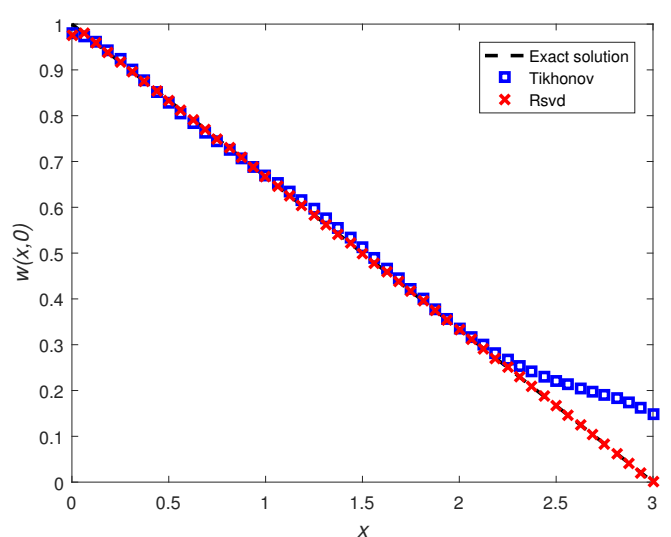


Fig. 25. The exact solution $w(x,0)$ and the MFS approximation with Tikhonov and rSVD established with $L=1.3$, $\alpha = 10^{-4}$, $k=30$, $M=26$ and $\delta=5\%$.

$$w_x^\delta(f(t), t) = -1 + N(0, \sigma^2), t \in (0, 1] \quad (51)$$

The dirichlet and neumann boundary conditions on the fixed boundary $x=0$ are as follows:

$$w(0, t) = -1 + \exp(t + 1), t \in [0, 1] \quad (52)$$

$$\frac{\partial w}{\partial x}(0, t) = -\exp(t + 1), t \in [0, 1] \quad (53)$$

We want to find the initial condition at $t=0$, which is given by

$$w(x, 0) = -1 + \exp(-x + 1), x \in [0, f(0)], f(0) = 1 \quad (54)$$

Figure 27 shows the MFS approximation for determining the initial condition using two regularization methods, rSVD and Tikhonov, additive noise 1%, and regularization parameter $\alpha=10^{-5}$.

Figure 29 shows the MFS approximation for determining the initial condition using two regularization methods, rSVD and Tikhonov, additive noise 3%, and regularization parameter $\alpha=10^{-5}$.

Figure 31 illustrates an MFS approximation to determine the initial condition using rSVD and Tikhonov regularization, with 5% additive noise, and the regularization parameter is $\alpha=10^{-5}$.

The results show that the rSVD regularization outperforms the Tikhonov regularization. We additionally observe that the MFS approximation becomes more accurate with the rSVD regularization when the additive noise increases.

Figures 28, 30, and 32 show how the rSVD regularization method performs to the Tikhonov method. We can see that employing MFS with the rSVD regularization method results in a smaller error than the exact solution. On the other hand, utilizing MFS with the Tikhonov reg-

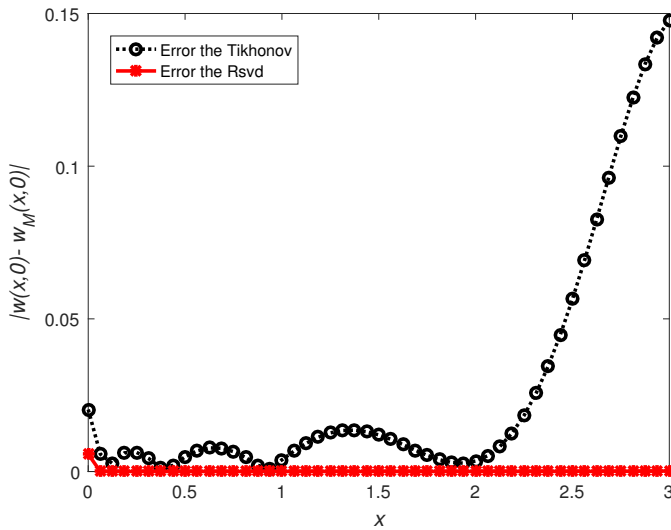


Fig. 26. Error between the exact solution $w(x,0)$ and the MFS approximation with Tikhonov and rSVD established with $\delta=5\%$.

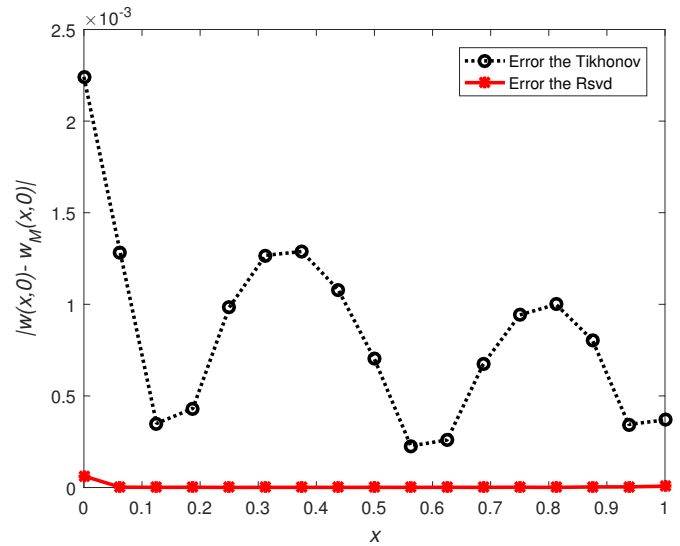


Fig. 28. Error between the exact solution $w(x,0)$ and the MFS approximation with Tikhonov and rSVD established with $\delta=1\%$.

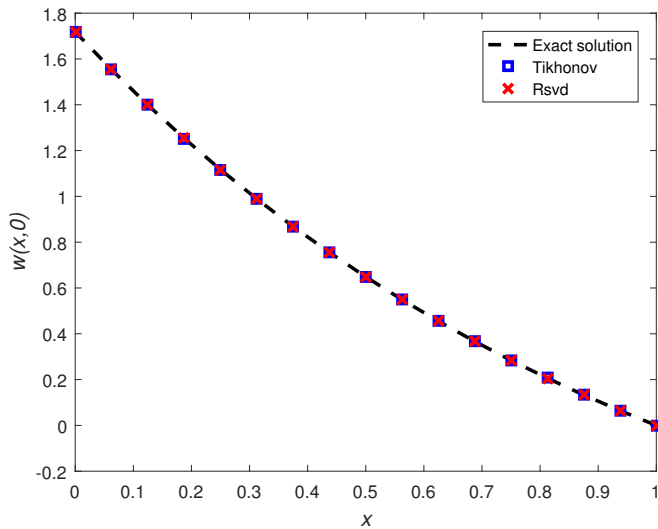


Fig. 27. The exact solution $w(x,0)$ and the MFS approximation with Tikhonov and rSVD established with $L=1.8$, $\alpha = 10^{-5}$, $k=30$, $M=16$ and $\delta=1\%$.

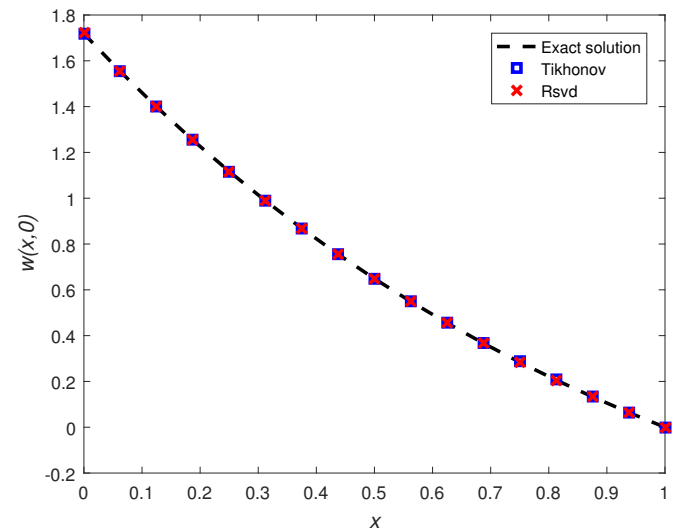


Fig. 29. The exact solution $w(x,0)$ and the MFS approximation with Tikhonov and rSVD established with $L=1.8$, $\alpha = 10^{-5}$, $k=30$, $M=16$ and $\delta=3\%$.

ularization method results in higher error than the exact solution. This performance is illustrated in all of these figures as the added noise increases.

VI. CONCLUSION

This paper introduces the Fundamental Solutions Method, which uses two methods of regularization to obtain the initial condition for the one-dimensional inverse Cauchy-Stefan problem. Our findings show that using MFS and rSVD regularization produces significantly more consistent and accurate results than Tikhonov regularization.

Numerical examples vividly demonstrate the effectiveness of MFS in solving the initial condition for the inverse Cauchy-Stefan problem. As part of our forthcoming research, we intend to explore the method precision and applicability across different problem classes, including direct problems, as well as two-dimensional inverse Cauchy-Stefan problems.

REFERENCES

- [1] L. I. Rubinstein, "The Stefan problem," *Translations of Mathematical Monographs*, Vol. 27, pp94-135, 1971
- [2] B. Tomas Johansson, D. Lesnic, and T. Reeve, "A method of fundamental solutions for the one-dimensional inverse Stefan problem," *Applied Mathematical Modelling*, vol. 35, no.9, pp4367-4378, 2011
- [3] B. Tomas Johansson, Daniel Lesnic, and Thomas Reeve, "The method of fundamental solutions for the two-dimensional inverse Stefan problem," *Inverse Problems in Science and Engineering*, vol. 22, no.1, pp112-129, 2014
- [4] B. Tomas Johansson, Daniel Lesnic, and Thomas Reeve "Numerical approximation of the one-dimensional inverse Cauchy-Stefan problem using a method of fundamental solutions," *Inverse Problems in Science and Engineering*, vol. 19, no.5, pp659-677, 2011
- [5] Sergio Andrés Ardila-Parra, Carmine Maria Pappalardo, Octavio Andrés González Estrada, and Domenico Guida, "Finite Element based Redesign and Optimization of Aircraft Structural Components using Composite Materials," *IAENG International Journal of Applied Mathematics*, vol. 50, no.4, pp860-877, 2020
- [6] Kanokwan Pananu, Surattana Sungnul, Sekson Sirisubtawee and Sutthisak Phongthanapanich, "Convergence and Applications of the Implicit Finite Difference Method for Advection-Diffusion-Reaction

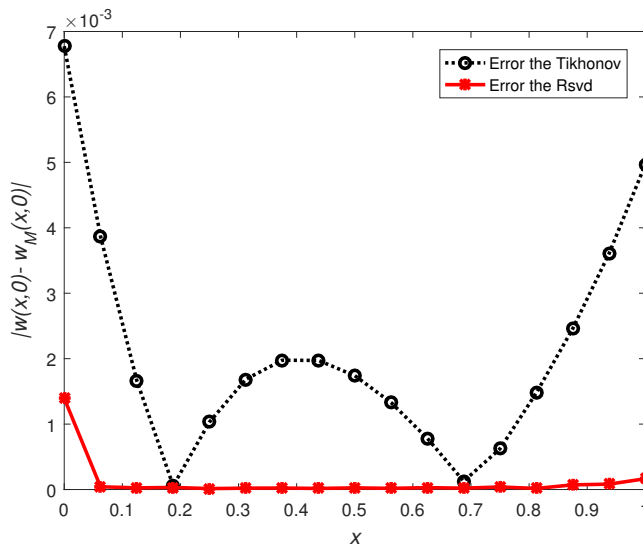


Fig. 30. Error between the exact solution $w(x,0)$ and the MFS approximation with Tikhonov and rSVD established with $\delta=3\%$.

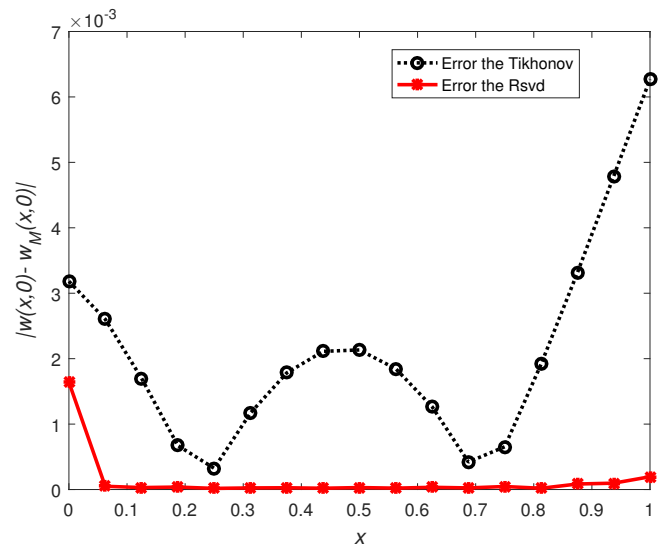


Fig. 32. Error between the exact solution $w(x,0)$ and the MFS approximation with Tikhonov and rSVD established with $\delta=5\%$.

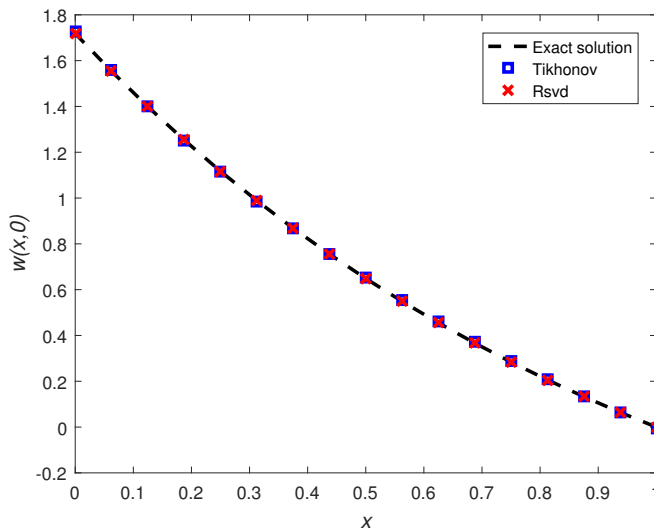


Fig. 31. The exact solution $w(x,0)$ and the MFS approximation with Tikhonov and rSVD established with $L=1.8$, $\alpha = 10^{-5}$, $k=30$, $M=16$ and $\delta=5\%$.

Equations," IAENG International Journal of Computer Science, vol. 47, no.4, pp645-663, 2020

[7] Supralee Chonladed, and Kanognudge Wuttanachamsri, "A Numerical Solution of Burger's Equation Based on Milne Method," IAENG International Journal of Applied Mathematics, vol. 51, no.2, pp411-415, 2021

[8] Erny Rahayu Wijayanti, Sumardi, and Nanang Susyanto, "European Call Options Pricing Numerically using Finite Element Method," IAENG International Journal of Applied Mathematics, vol. 52, no.4, pp940-945, 2022

[9] Mohammed Baati, Nada Chakhim, Mohamed Louzar, and Abdellah Lamni, "Numerical Approximation of the One-dimensional Inverse Stefan Problem Using a Meshless Method," Engineering Letters, vol. 32, no. 1, pp112-122, 2024

[10] S. Chantasiriwan, B.Tomas Johansson, and D. Lesnic, "The method of fundamental solutions for free surface problem," Engineering Analysis with Boundary Elements, vol. 33, no.4, pp529-538, 2009

[11] B. Tomas Johansson, Daniel Lesnic, and Thomas Reeve, "The method of fundamental solutions for the two-dimensional inverse Stefan problem," Inverse Problems in Science and Engineering, vol. 22, no.1, pp112-129, 2014

[12] M. Gu, "Subspace iteration randomization and singular value problems," SIAM Journal on Scientific Computing, vol. 37, no.3, ppA1139-

A1173, 2015

[13] Rafi Witten and Emmanuel Candès, "Randomized algorithms for low-rank matrix factorizations: sharp performance bounds," Algorithmica, vol. 72, no.1, pp264-281, 2015

[14] J. R. Cannon and C. Denson Hill, "Existence, uniqueness, stability, and monotone dependence in a Stefan problem for the heat equation," Journal of Mathematics and Mechanics, vol. 17, no.1, pp1-19, 1967

[15] N. L. Gol'dman, "Inverse Stefan Problem," Kluwer Academic Publishers, 1997

[16] B. Tomas Johansson, and Daniel Lesnic, "A method of fundamental solutions for transient heat conduction," Engineering Analysis with Boundary Elements, vol. 32, no.9, pp697-703, 2008

[17] B. Tomas Johansson, and Daniel Lesnic, "A method of fundamental solutions for transient heat conduction in layered materials," Engineering Analysis with Boundary Elements, vol. 33, no.12, pp1362-1367, 2009

[18] C.S. Chen, Hokwon A. Cho, M. A. Golberg, "Some comments on the ill-conditioning of the method of fundamental solutions," Engineering Analysis with Boundary Elements, vol. 30, no.5, pp405-410, 2006

[19] P. A. Ramachandran, "Method of fundamental solutions: singular value decomposition analysis," Communications in Numerical Methods in Engineering, vol. 18, no.11, pp789-801, 2002

[20] Jingjing Cui, Guohua Peng, Quan Lu, and Zhengge Huang, "Special Regularized HSS Iteration Method for Tikhonov Regularization," IAENG International Journal of Applied Mathematics, vol. 50, no.2, pp359-372, 2020

[21] Per Christian Hansen, "Analysis of discrete ill-posed problems by means of the L-curve," Society for Industrial and Applied Mathematics, vol. 34, no.4, p561-580, 1992

[22] Per Christian Hansen, "The truncated SVD as a method for regularization," BIT Numerical Mathematics, vol. 27, no.4 pp534-553, 1987

[23] Kazufumi Ito and Bangti Jin, "Regularized Linear Inversion with Randomized Singular Value Decomposition," Mathematical and Numerical Approaches for Multi-Wave Inverse Problems, vol. 328, pp45-72, 2019

[24] Xingyu Tuo, Yin Zhang, Yingying Wang, Deqing Mao, Yongchao Zhang, and Yulin Huang, "A Fast Angle Super-resolution Imaging Method for Airborne Scanning Radar based on rSVD," 2019 International Radar Conference (RADAR), pp1-5, 2019

[25] Jean-Luc Chabert, "Gauss et la méthode des moindres carrés," Revue d'histoire des sciences, vol. 42, no.1, pp5-26, 1989

[26] Diego A. Murio, "Solution of inverse heat conduction problems with phase changes by the mollification method," Computers and Mathematics with Applications, vol. 24, no.7, pp45-57, 1992

[27] G. M. M. Reddy, M. Vynnycky, and J. A. Cuminato, "On efficient reconstruction of boundary data with optimal placement of the source points in the MFS: application to inverse Stefan problems," Inverse Problems in Science and Engineering, vol. 26, no.9, pp1741-5977, 2017